BASIC SCIENCES

PHYSICS AND RADIATION BIOLOGY

Correction for Out-of-Focal-Plane Blurring in a Simulated Multiplane Tomographic Scanner

H. R. Hooper, J. W. Scrimger, and B. C. Lentle

Cross Cancer Institute, Edmonton, Alberta, Canada

A technique has been developed to remove out-of-focal-plane blurring from coronal and axial images made using a multiplane tomographic scanner. The technique uses a combined smoothing and differential operator that is applied to the axial images. It has been tested using computer-simulated images, with favorable results. The usefulness of the technique in a real system has yet to be determined.

J Nucl Med 20:1194–1196, 1979

Since its initial development (*1,2*) the multiplane tomographic scanner has proved to be a useful clinical tool, providing coronal images of superior diagnostic quality (*3–6*). An inherent problem with the scanner, however, is that, although activity in specified coronal planes can be sharply focused and activity in other planes blurred, the out-of-focus activity is still superimposed on the focused planes. This out-of-focal-plane blurring is evident clinically on liver scans, where lesions in a given liver plane may be obscured by overlying activity (*3*).

Interest has developed (*7,8*) in the use of a multiplane tomographic scanner combined with a computer to provide axial and other sectional images as well as those in the coronal plane. Axial imaging would be helpful both because it could provide better information on the depth distribution of radiotracer in the body, and because the gamma images produced could be compatible with transmission CT images. Out-of-focal-plane blurring will appear on axial images as two cones of activity meeting at each source location, with the cone's apical angle equal to the acceptance angle of the collimator used (*7*).

Out-of-focal-plane blurring results from the use of back projection in the reconstruction of images. The two cones of activity noted in axial imaging are in fact a truncated "star" artifact similar to the star artifact observed in CT systems using back projection (*9*). Conventional techniques, such as filtered back-projection or iterative reconstruction, have been used to correct this artifact in a limited-geometry system. For a multiplane tomographic scanner, however, these techniques—and in particular filtered back projection—can require a considerable amount of computer processing time. A faster reconstruction technique would be desirable.

In order to study out-of-focal-plane blurring, a computer program has been written to simulate axial image reconstruction in an ideal multiplane tomographic scanner. A technique has been developed to correct for out-of-focal-plane blurring in axial images in such a scanner, and the technique tested on simulated images. Blur correction in coronal planes is automatic provided the technique is applied to all axial planes. Testing of the technique in practice is continuing.

DERIVATION

A three-dimensional image, $g(\vec{r})$, produced by a source distribution, $f(\vec{r})$, can be expressed in terms of the integral equation

$$g(\vec{r}) = \int F(\vec{r},\vec{r}')\, f(\vec{r}')\, d\vec{r}'$$

where $F(\vec{r},\vec{r}')$ is the point-source response function for a source at $\vec{r}'$. If the function $F(\vec{r},\vec{r}')$ can be expressed in terms of the difference between $\vec{r}$ and $\vec{r}'$, then

Received March 20, 1979; revision accepted June 7, 1979.

For reprints contact: H. R. Hooper, Dept. of Nuclear Medicine, Cross Cancer Institute, 11560 University Ave., Edmonton, Alberta, Canada T6G 1Z2.

$$F(\bar{r},\bar{r}') = F(\bar{r} - \bar{r}'),$$

and the source distribution $f(\bar{r})$ can be determined from the image distribution $g(\bar{r})$ using the linear differential operator D defined such that (*10*)

$$D\, F(\bar{r} - \bar{r}') = \delta(\bar{r} - \bar{r}'),$$

in which case

$$f(\bar{r}) = D\, g(\bar{r}).$$

The validity of writing $F(\bar{r},\bar{r}')$ as $F(\bar{r} - \bar{r}')$ will be discussed below.

The form of the operator D will depend on the symmetries of the function $F(\bar{r} - \bar{r}')$. If we define three mutually orthogonal axes x, y, and z such that the z axis is perpendicular to the coronal plane, the x axis perpendicular to the cross-sectional plane, and the y axis perpendicular to the sagittal plane, then for most multiplane tomographic scanners $F(\bar{r} - \bar{r}')$ is symmetric about the line $x = x'$, $y = y'$. D must therefore also be symmetric in all coronal planes about this line.

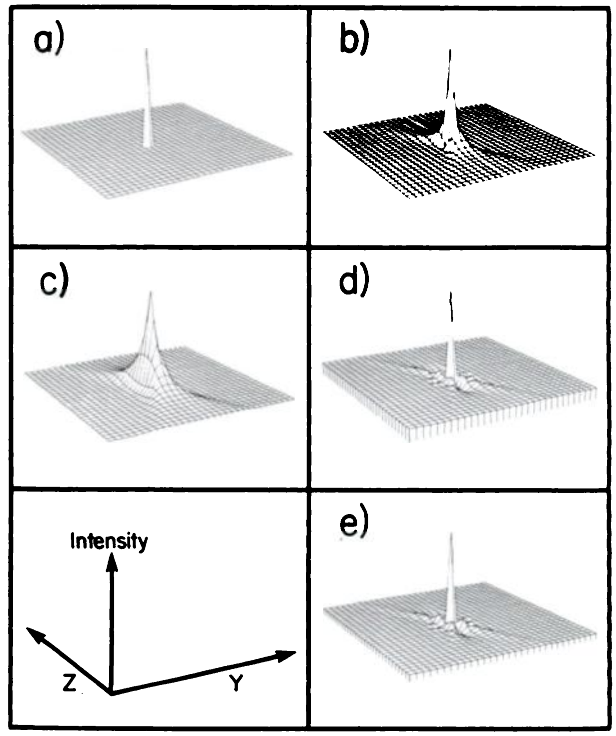

FIG. 1. Perspective drawings illustrating correction technique for out-of-focal-plane blurring. (A) Location of a point source in cross-sectional plane. (B) Point-source response function $F(\bar{r} - \bar{r}')$ for source in (a). (C) $F(\bar{r} - \bar{r}')$ after smoothing in y and x directions. (D) $DS\, F(\bar{r} - \bar{r}')$. (E) $E\, F(\bar{r} - \bar{r}')$.

COMPUTER SIMULATIONS

A program was written to simulate the operation of an "ideal" multiplane tomographic scanner. The simulations were ideal in that both the channel component of the point-source response function and the intrinsic resolution of the detector were considered to be negligible, and thus $F(\bar{r} - \bar{r}')$ was determined solely by parallax (*1*). Under these conditions $F(\bar{r} - \bar{r}')$ is symmetrical about the point $\bar{r} = \bar{r}'$ and D can contain only even-order differential terms. Figure 1A shows the location of a point source in a cross-sectional plane. This perspective diagram is a representation of the function $\delta(\bar{r} - \bar{r}')$. The function $F(\bar{r} - \bar{r}')$ for an ideal scanner with an acceptance angle of 60° is shown in Fig. 1B.

Taking into account the constraints on D noted above, the simplest nontrivial form that D can take is

$$D = \frac{\partial^2}{\partial z^2}$$

If this D is applied to $F(\bar{r} - \bar{r}')$, however, the result is a poor approximation of the delta function $\delta(\bar{r} - \bar{r}')$. Higher-order derivatives could be added to D to improve the representation, but this is in fact difficult both because the number of terms to be added could be quite large and because, in any practical situation, the derivatives must be determined numerically.

An alternate approach becomes apparent if $F(\bar{r} - \bar{r}')$ is studied closely. Note that $F(\bar{r} - \bar{r}')$ changes rapidly with y (and x) about the point $r = r'$. This rapid fluctuation in x and y is one of the reasons why $D\, F(\bar{r} - \bar{r}')$ is a poor approximation for $\delta(\bar{r} - \bar{r}')$. It might be reasonable, therefore, to try smoothing $F(\bar{r} - \bar{r}')$ first, in the x and y directions, using a linear smoothing operator S, and then to modify this function with D. Figure 1C shows such a smoothed function $S\, F(\bar{r} - \bar{r}')$, while Fig. 1D shows the function $DS\, F(\bar{r} - \bar{r}')$. Some of the negative portions of Fig. 1D can be compensated for by adding the original $F(\bar{r} - \bar{r}')$ (Fig. 1B) to $DS\, F(\bar{r} - \bar{r}')$. Fig. 1E shows the results of operating on $F(\bar{r} - \bar{r}')$ with the operator $E = a + b\, DS$, where a and b are constants. The components of the operator S and the constants a and b have been optimized so that Fig. 1E most closely approximates a δ function. The operator S takes the form

$$S = \begin{matrix} 0.00 & 0.00 & 0.08 & 0.00 & 0.00 \\ 0.00 & 0.20 & 0.36 & 0.20 & 0.00 \\ 0.08 & 0.36 & 1.00 & 0.36 & 0.08 \\ 0.00 & 0.20 & 0.36 & 0.20 & 0.00 \\ 0.00 & 0.00 & 0.08 & 0.00 & 0.00 \end{matrix}$$

while the constants a and b are: $a = 0.12$; and $b = 1.00$. E is a linear operator and can thus be used to calculate $f(\bar{r})$ from $g(\bar{r})$.

Figure 2 shows two examples of axial imaging in which $f(\bar{r})$ is reconstructed from $g(\bar{r})$ using the equation $f(\bar{r}) = E\, g(\bar{r})$. In this figure, images are shown on a 32 × 32 matrix with a 16-level gray scale. The example on the left side of Fig. 2 simulates a three-dimensional cross

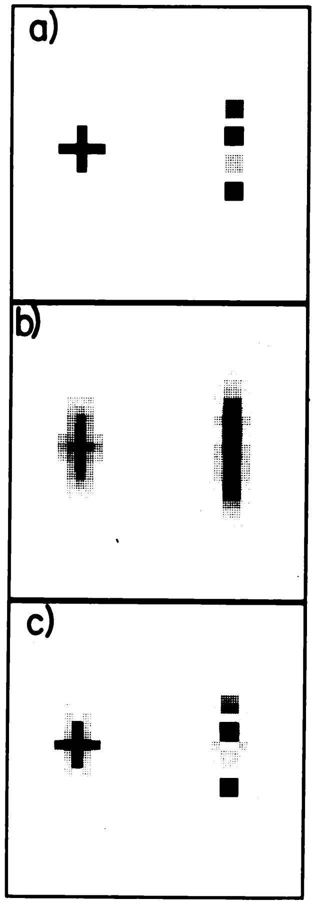

FIG. 2. Examples of simulated axial images before and after correction for out-of-focal-plane blurring. (A) Location of sources in cross-sectional plane. Source distribution on left is three-dimensional cross of activity with arms of equal length in y, z, and, hidden in this view, x directions. (B) Distorted images reconstructed using back projection. (C) Images corrected for out-of-focal-plane blurring.

of activity with arms of equal length in the y, z, and, hidden in this view, x directions. The example on the right side of Fig. 2 simulates four sources of varying strengths aligned in the z direction. In both examples the images that have been corrected for out-of-focal-plane blurring (C) are a considerable improvement on the uncorrected images (B).

DISCUSSION

The approximation, made earlier, that $F(\vec{r},\vec{r}')$ can be rewritten as $F(\vec{r} - \vec{r}')$ will not in general be true for a real multiplane tomographic scanner. In addition to a parallax component, $F(\vec{r},\vec{r}')$ is determined by a collimator channel component and by an intrinsic focused collimator and detector resolution component (*1*), neither of which is a function of $\vec{r} - \vec{r}'$. $F(\vec{r},\vec{r}')$ is also affected by photon scatter. Just how much $F(\vec{r},\vec{r}')$ deviates from $F(\vec{r} - \vec{r}')$, and how sensitive an operator such as E is to $F(\vec{r},\vec{r}')$ must be determined experimentally. Note that since E contains a smoothing operator, S, E may not be too sensitive to $F(\vec{r},\vec{r}')$.

Another characteristic of real scanners, which was not included in the computer simulations, is the presence of noise. Since the derivatives used in the correction routine must be calculated numerically, the presence of noise might present problems when such a technique is applied in practice. Smoothing may decrease the effects of noise, but again experimentation will be necessary to determine the overall effect that noise has on image correction.

In conclusion, a technique has been developed to remove out-of-focal-plane blurring from images made using a multiplane tomographic scanner. The feasibility of the technique has been demonstrated for simple computer-simulated images, but the final usefulness of the technique in practice has yet to be determined.

ACKNOWLEDGMENT

This work was supported by Alberta Heritage Trust Cancer Research Fund.

REFERENCES

1. ANGER HO: Tomographic gamma-ray scanner with simultaneous readout of several planes. In *Fundamental Problems in Scanning*, Gottschalk A, Beck RN, eds. Springfield, IL, Thomas Books, 1968, pp 195-211
2. ANGER HO: Multiplane tomographic gamma-ray scanner. In *Medical Radioisotope Scintigraphy*, I. Vienna, IAEA, 1969, pp 203-216
3. VOLPE JA, MCRAE J, ANGER HO: Clinical experience with the multiplane tomographic scanner. *J Nucl Med* 12: 101-106, 1971
4. TURNER DA, RAMACHANDRAN PC, ALI AA, et al: Brain scanning with the Anger multiplane tomographic scanner as a primary examination. *Radiology* 121: 125-129, 1976
5. TURNER DA, FORDHAM EW, PAGANO JV, et al: Brain scanning with the Anger multiplane tomographic scanner as a second examination. *Radiology* 121: 115-124, 1976
6. SHIMSHAK RR, KOROBKIN M, HOFFER PB, et al: The complementary role of gallium citrate imaging and computed tomography in the evaluation of suspected abdominal infection. *J Nucl Med* 19: 262-269, 1978
7. GARCIA EV, INGLIS AE, DIAZ JE, et al: Longitudinal and transverse single-photon emission computed body tomography using an Anger tomographic scanner. *J Nucl Med* 19: 708, 1978 (abst)
8. SILVERSTEIN EA, CHUNG-BIN A, WACHTOR T, et al: Digital-computer data acquisition and image reconstruction for a PHO/CON tomographic scanner. *Med Imag* 2: 44, 1977 (abst)
9. BROOKS RA, DICHIRO G: Principles of computer assisted tomography (CAT) in radiographic and radioisotopic imaging. *Phys Med Biol* 21: 689-732, 1976
10. BUTKOV E: *Mathematical Physics*. Reading, MA, Addison-Wesley Publishing Co., 1968, pp 503-552